Kinetics of the $CH_2Cl + CH_3$ and $CHCl_2 + CH_3$ Radical−Radical Reactions

Alexander A. Shestov,† Konstantin V. Popov,‡ and Vadim D. Knyazev*

Research Center for Chemical Kinetics, Department of Chemistry, The Catholic University of America, Washington, DC 20064

Received: February 18, 2005; In Final Form: May 2, 2005

The $CH_2Cl + CH_3$ (1) and $CHCl_2 + CH_3$ (2) cross-radical reactions were studied by laser photolysis/photoionization mass spectroscopy. Overall rate constants were obtained in direct real-time experiments in the temperature region 301−800 K and bath gas (helium) density $(6-12) \times 10^{16}$ atom cm^{-3}. The observed rate constant of reaction 1 can be represented by an Arrhenius expression $k_1 = 3.93 \times 10^{-11}$ exp(91 K/T) cm^3 molecule^{-1} s^{-1} (±25%) or as an average temperature-independent value of $k_1 = (4.8 \pm 0.7) \times 10^{-11}$ cm^3 molecule^{-1} s^{-1}. The rate constant of reaction 2 can be expressed as $k_2 = 1.66 \times 10^{-11}$ exp(359 K/T) cm^3 molecule^{-1} s^{-1} (±25%). C_2H_4 and C_2H_3Cl were detected as the primary products of reactions 1 and 2, respectively. The experimental values of the rate constant are in reasonable agreement with the prediction based on the "geometric mean rule." A separate experimental attempt to determine the rate constants of the high-temperature $CH_2Cl + O_2$ (10) and $CHCl_2 + O_2$ (11) reaction resulted in an upper limit of 1.2×10^{-16} cm^3 molecule^{-1} s^{-1} for k_{10} and k_{11} at 800 K.

I. Introduction

Radical−radical cross-combination reactions constitute an integral part of the overall mechanisms of oxidation and pyrolysis of hydrocarbons.[1,2] Reactions of chlorinated methyl radicals with other radicals are important in the mechanisms of combustion of chlorinated hydrocarbons. When compared to nonchlorinated radicals, chlorinated methyl radicals are characterized by increased kinetic stability in the combustion environment because of the weaker C−O bonds in the peroxy adducts that are formed by the addition of the radical to the O_2 molecule (ref 3 and references therein). These weaker C−O bonds favor decomposition to O_2 and the chlorinated methyl radical as opposed to further transformations of the adduct. Thus, high-temperature reactions between chloromethyl radicals and O_2 are relatively slow, and consequently, these radicals tend to accumulate in higher concentrations in flames, resulting in a greater importance of their reactions with other open-shell species, such as O, OH, hydrocarbon radicals, and H atoms.[4] In the oxidation and pyrolysis of pure chlorinated methanes, the reactions between chlorinated methyl radicals are the major pathways to higher molecular mass products (C_2, C_3, etc.). In more complex systems involving oxidation of mixtures of methane/chlorinated methane (for example, $CH_2Cl_2/CH_4/O_2$/Ar mixtures[5]), reactions between chlorinated methyl radicals and CH_3 become important and play the same role in molecular mass growth.[5−8]

Reliable knowledge of the rate constants of the chloromethyl + CH_3 reactions is needed to accurately predict high-molecular-mass product formation (including toxic byproducts) in the combustion and pyrolysis of chlorinated hydrocarbons. Despite the importance and sensitivity of these reactions, very little experimental information on them is available in the literature. The reaction of the trichloromethyl radical (CCl_3) with CH_3 is the only reaction of this class that has been studied experimentally. One room-temperature study[9,10] reported an anomalously low upper limit value of 6×10^{-12} cm^3 molecule^{-1} s^{-1}; our recent investigation[11] of this reaction in the 306−800-K temperature range, however, resulted in a larger value of $(2.05 \pm 0.30) \times 10^{-11}$ cm^3 molecule^{-1} s^{-1} for the rate constant of the $CCl_3 + CH_3$ reaction, independent of temperature. Although this value is larger than that of refs 9 and 10, it is still considerably lower than those obtained earlier for a series of reactions of polyatomic hydrocarbon radicals with CH_3,[12−14] which generally are in the $(0.9-1.2) \times 10^{-10}$ cm^3 molecule^{-1} s^{-1} range at room temperature.

In the current study, we continue our experimental studies of the reactions of chlorinated methyl radicals with CH_3 by investigating the kinetics of the two remaining reactions belonging to this class

$$CH_2Cl + CH_3 \rightarrow \text{products} \quad (1)$$

$$CHCl_2 + CH_3 \rightarrow \text{products} \quad (2)$$

Reactions 1 and 2 were studied by means of laser photolysis/photoionization mass spectrometry at low bath gas densities ([He] = $(6-12) \times 10^{16}$ atom cm^{-3}) in the 301−800-K temperature range. For each reaction, overall rate constants were obtained in direct experiments by monitoring the real-time kinetics of both the R and the CH_3 radical (R = CH_2Cl, $CHCl_2$). The mechanisms of these reactions are expected to be those of addition−elimination, producing HCl and a matching olefin (see below); thus, the obtained rate constant values are those of the high-pressure limit. In a separate experimental investigation of the high-temperature reactions between CH_2Cl and O_2 and $CHCl_2$ and O_2, upper limits of the rate constants were obtained at 800 K.

* To whom correspondence should be addressed. E-mail: knyazev@cua.edu.

† Current address: Center for Magnetic Resonance Research, University of Minnesota, Minneapolis, MN 55455.

‡ On leave from the Higher Chemical College of the Russian Academy of Sciences, Miusskaya sq, 9, Moscow 125190, Russia.

10.1021/jp050863k CCC: $30.25
Published on Web 06/22/2005

This article is organized as follows. Section I is an introduction. Section II presents the experimental method and the results. A discussion is given in section III.

II. Experimental Section

Apparatus. Details of the experimental apparatus[15] and method[11−14] have been described previously. Only a brief description is presented here. Pulsed 193-nm unfocused collimated radiation from a Lambda Physik 201 MSC ArF excimer laser was directed along the axis of a 50-cm-long 1.05-cm inside diameter (i.d.) heatable tubular quartz reactor coated with boron oxide.[16] The laser was operated at 4 Hz; the energy flux of the laser radiation inside the reactor was in the range of 8−44 mJ/cm^2 per pulse depending on the degree of laser beam attenuation.

Gas flowing through the tube at ~4 m s^{-1} (in order to replace the photolyzed gas with a fresh reactant gas mixture between the laser pulses) contained free radical precursors in low concentrations and the bath gas, helium. The gas was continuously sampled through a 0.04-cm-diameter tapered hole in the wall of the reactor (gas-sampling orifice) and formed into a beam by a conical skimmer (0.15 cm i.d.) before it entered the vacuum chamber containing the photoionization mass spectrometer (PIMS). As the gas beam traversed the ion source, a portion was photoionized using an atomic resonance lamp, mass selected in an EXTREL quadrupole mass filter, and detected by a Daly detector.[17] Temporal ion signal profiles were recorded from 20 ms before each laser pulse to 25 ms following the pulse by using a multichannel scaler. Typically, data from 500 to 10000 repetitions of the experiment were accumulated before the data were analyzed. The sources of ionizing radiation were chlorine (8.9−9.1 eV, CaF_2 window, used to detect CH_2Cl, $CHCl_2$, C_2H_5, and CH_3CHCl), hydrogen (10.2 eV, MgF_2 window, used to detect CH_3, C_2H_3Cl, and $(CH_3)_2CO$), and argon (11.6−11.9 eV, LiF window, used to detect CH_3CH_2Cl, CH_3CHCl_2, and C_2H_4) resonance lamps.[18]

Photolysis of Radical Precursors. Radicals were produced by the 193-nm photolysis of corresponding precursors. The photolysis of acetone at 193 nm, which was used in this study as the source of methyl radicals, was shown by Lightfoot et al.[19] to proceed predominantly (>95%) via channel 3a under conditions similar to those used in the current work.

$$CH_3C(O)CH_3 \xrightarrow{193\ nm} 2CH_3 + CO \quad (3a)$$

$$\rightarrow H + CH_2C(O)CH_3 \quad (3b)$$

$$\rightarrow CH_4 + CH_2CO \quad (3c)$$

Photolysis channels 3b and 3c are known[19] to occur to a minor degree, <3 and <2%, respectively. The initial concentration of CH_3 radicals produced by the photolysis can thus be determined by measuring the photolytic depletion of $CH_3C(O)CH_3$, i.e., the fraction of acetone decomposed due to photolysis (see below).

Chloromethyl and dichloromethyl radicals were produced in photolysis of dichloromethane and chloroform, respectively

$$CH_2Cl_2 \xrightarrow{193\ nm} CH_2Cl + Cl \quad (4a)$$

$$\rightarrow \text{other products} \quad (4b)$$

$$CHCl_3 \xrightarrow{193\ nm} CHCl_2 + Cl \quad (5a)$$

$$\rightarrow \text{other products} \quad (5b)$$

Radical precursors were obtained from Aldrich (acetone, >99.9%; CH_2Cl_2, ≥99.9%; $CHCl_3$, ≥99.99%) and were purified by vacuum distillation prior to use. Helium (>99.999%, <1.5 ppm of O_2, MG Industries) was used without further purification.

Method of Determination of Rate Constants. CH_3 and R radicals (R = CH_2Cl or $CHCl_2$) were produced simultaneously by the 193-nm photolysis of a mixture of corresponding precursors highly diluted in the helium carrier gas (>99.9%). The rate constant measurements were performed using a technique analogous to that applied by Niiranen and Gutman to the studies of the $SiH_3 + CH_3$ and $Si(CH_3)_3 + CH_3$ kinetics,[20] which is a further development of the method used by Garland and Bayes to study a series of radical cross-combination reactions.[10] Experimental conditions (in particular, the two precursor concentrations) were selected to create a large excess of initial concentrations of methyl radicals over the total combined concentration of all the remaining radicals formed in the system. The initial concentration of methyl radicals was always 9−132 times higher than that of R; the average $[CH_3]_0/[R]_0$ ratio was 57. The concentration of R radicals was always less than 1.4×10^{11} molecule cm^{-3}. Under these conditions, the self-recombination of methyl radicals was essentially unperturbed by the presence of the other radicals due to the low concentrations of the latter. At the same time, the kinetics of R decay was completely determined by the reaction with CH_3 and unaffected either by self-reaction or by reactions with other active species formed in the system, such as the side products of precursor photolysis, because of the low concentrations of all radicals other than methyl.

Heterogeneous loss was the only additional sink of methyl and R radicals that had to be taken into account. Thus, the kinetic mechanism of the important loss processes of CH_3 and R in these experiments is as follows

$$R + CH_3 \rightarrow \text{products} \quad (1 \text{ or } 2)$$

$$CH_3 + CH_3 \rightarrow C_2H_6 \quad (6)$$

$$R \rightarrow \text{heterogeneous loss} \quad (7 \text{ or } 8)$$

$$CH_3 \rightarrow \text{heterogeneous loss} \quad (9)$$

(Here, reactions 7 and 8 are the wall losses of CH_2Cl and $CHCl_2$, respectively). For this mechanism and for the initial conditions described above, the system of first order differential equations can be solved analytically

$$\frac{[CH_3]_t}{[CH_3]_0} = \frac{k_9 \exp(-k_9 t)}{2k_6[CH_3]_0(1 - \exp(-k_9 t)) + k_9} \quad (I)$$

$$\frac{[R]_t}{[R]_0} = \exp(-k_W t)\left[\frac{k_9}{2k_6[CH_3]_0(1 - \exp(-k_9 t)) + k_9}\right]^{kR[CH_3]_0/2k_6[CH_3]_0} \quad (II)$$

The variables k_R and k_W in eq II have the meanings of the rate constant of the R + CH_3 reaction ($k_R = k_1$ or k_2) and that of the R radical wall loss ($k_W = k_7$ or k_8).

Experimental signal profiles of CH_3 and R radicals (see subsection Procedure below) were fitted with eqs I and II, respectively, to obtain the values of the $k_6[CH_3]_0$ and $k_R[CH_3]_0$ products. The k_R rate constants (i.e., k_1 and k_2) were then obtained by dividing the experimental $k_R[CH_3]_0$ values by $[CH_3]_0$

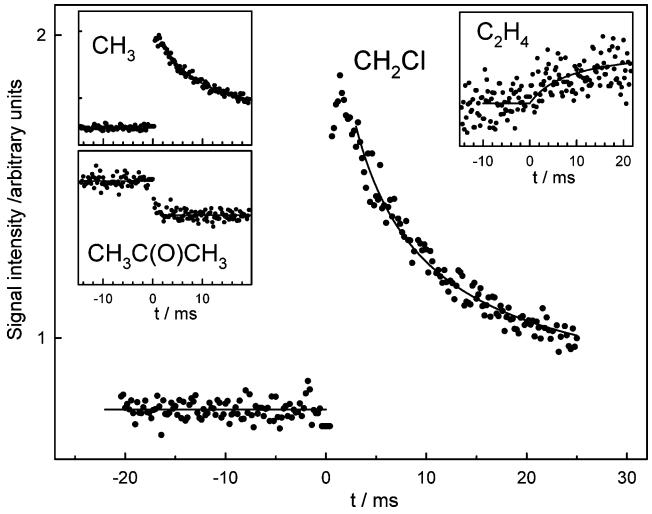

Figure 1. Example of a temporal ion signal profile of CH_2Cl obtained in the experiments to determine k_1. Insets: profiles of CH_3, $CH_3C(O)CH_3$, and C_2H_4 obtained in the same experiment. $T = 301$ K, [He] $= 1.20 \times 10^{17}$, $[CH_2Cl_2] = 1.29 \times 10^{13}$, $[CH_3C(O)CH_3] = 8.52 \times 10^{12}$, $[CH_2Cl]_0 \leq 1.4 \times 10^{11}$, $[CH_3]_0 = 1.28 \times 10^{12}$ molecule cm^{-3}.

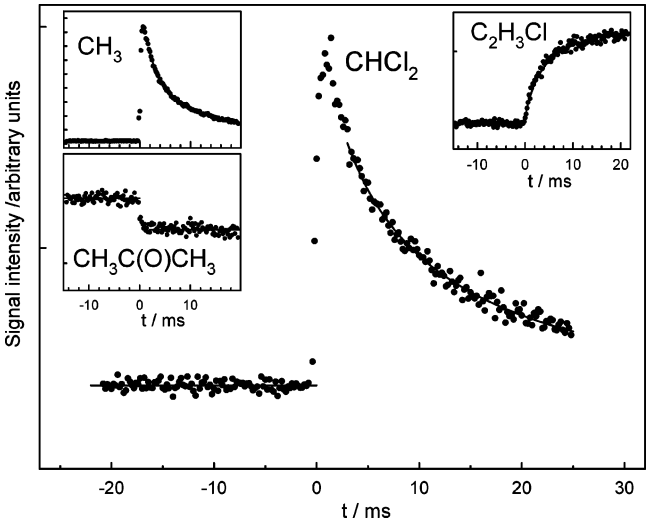

Figure 2. Example of a temporal ion signal profile of $CHCl_2$ obtained in the experiments to determine k_1. Insets: profiles of CH_3, $CH_3C(O)CH_3$, and C_2H_3Cl obtained in the same experiment. $T = 304$ K, [He] $= 6.0 \times 10^{16}$, $[CHCl_3] = 1.51 \times 10^{13}$, $[CH_3C(O)CH_3] = 3.80 \times 10^{13}$, $[CHCl_2]_0 \leq 6.8 \times 10^{10}$, $[CH_3]_0 = 4.07 \times 10^{12}$ molecule cm^{-3}.

determined by measuring the photolytic depletion of acetone (see below). An important feature of this method is that exact knowledge of the initial concentration of R is not required for the determination of the rate constants. In this respect, the approach is similar to the pseudo-first-order method frequently applied to studies of kinetics of second-order reactions.

Procedure. In experiments with only one of the radical precursors present in the reactor under conditions where radical−radical reactions are negligible (low precursor concentration and/or low laser intensity), the radical kinetics (CH_3, CH_2Cl, or $CHCl_2$) was that of purely exponential decay, attributed to heterogeneous loss processes. The rate constants of heterogeneous loss of CH_2Cl and $CHCl_2$ radicals ($k_W = k_7$ or k_8) were determined in separate sets of measurements.

In the experiments to measure the R + CH_3 reaction rate constants, the initial (high) concentration of methyl radicals was determined by measuring the photolytic depletion of acetone (the fraction of acetone decomposed due to photolysis). The value of the decomposition ratio (the relative decrease in the precursor concentration upon photolysis) was obtained directly from the acetone ion signal profile (Typical profiles are shown in Figures 1 and 2.). Initial concentrations of R were evaluated by monitoring the photolytic depletion of corresponding precursors. Since products other than R were also produced in the photolysis (reactions 4 and 5), only upper limit values to the concentration of R could be obtained.

The procedure of determination of the R + CH_3 rate constants for each set of experimental conditions consisted of the following sequence of measurements:

1. Kinetics of heterogeneous loss of R (determination of k_W). Only the R radical precursor is present in the reactor (along with the helium carrier gas, which is always present).

2. Decomposition ratio of acetone (determination of $[CH_3]_0$). Both radical precursors are in the reactor, from here to step 4.

3. Kinetics of methyl radical decay (determination of the $k_6[CH_3]_0$ product and k_9).

4. Kinetics of R radical decay in the presence of methyl radicals (determination of the $k_R[CH_3]_0$ product and k_R.

Measurements 2 and 3 were repeated in reverse order after monitoring the kinetics of R radicals in the presence of methyl radicals in order to ensure the stability of initial concentrations of CH_3. Also, the stability of the heterogeneous loss rate constants during the set of measurements was checked experimentally.

Typical temporal profiles of $[CH_3C(O)CH_3]$ (photolytic precursor of CH_3 radicals), $[CH_3]$, and [R] are shown in Figures 1 and 2. The lines through the experimental $[CH_3]$ and [R] vs time profiles were obtained from fits of these dependences with expressions I and II, respectively. In the data fitting, the first three milliseconds of the [R] vs time profiles were not used to ensure that radial diffusion of R (resulting in short but nonzero growth times of R signals following the precursor photolysis, see Figures 1 and 2 and discussion in ref 11) has no influence on the derived rate constant values. In each experiment (consisting of the set of measurements described above), the values of the $k_6[CH_3]_0$ product and k_9 were obtained from the fit of the $[CH_3]$ vs time dependence (measured in step 3). Then the value of the $k_R[CH_3]_0$ product was obtained from the fit of the [R] vs time dependence using the k_W, k_9, and $k_6[CH_3]_0$ values obtained in steps 1 and 3. Finally, the value of k_R ($k_R = k_1$ or k_2) was obtained by dividing the $k_R[CH_3]_0$ product by $[CH_3]_0$ determined in step 2.

In principle, it was possible to obtain the values of k_9 in separate experiments with low initial CH_3 concentrations selected in such a way as to make the rates of methyl self-reaction negligible. However, such a procedure, although more involved, would not provide better accuracy in determination of k_R, as it is the overall quality of the fit of equation I to the $[CH_3](t)$ signal that is important for correct description of the R decay kinetics, not the accuracy of individual k_6 and k_9 parameters. Separate experiments with low CH_3 concentrations were performed periodically to confirm that the values of k_9 obtained are in general agreement with those derived from the fits of CH_3 decays obtained with high methyl radical concentrations.

The sources of error in the measured experimental parameters were subdivided into statistical and systematic and propagated to the final values of the rate constants using different mathematical procedures for propagating systematic and statistical uncertainties.[21] In particular, the effects of uncertainties in the heterogeneous radical decay rates and in the $k_6[CH_3]_0$ product on the derived k_1 and k_2 values were evaluated for all

TABLE 1: Conditions and Results of Experiments to Determine the Rate Constants k_1 of the $CH_2Cl + CH_3$ Reaction

T/K	[He][a]	$[CH_2Cl_2]$[b]	$[C_3H_6O]$[b]	$[CH_2Cl]_0$ [b]	$[CH_3]_0$ [b]	I[c]	k_7/s^{-1}	k_9/s^{-1}[d]	$k_6[CH_3]_0/s^{-1}$	k_1 [e]
301	12.0	129	85	1.4	12.8	44	44.2	0.0	58.3	4.56 ± 1.67
301	12.0	126	180	1.4	28.4	44	50.7	6.5	161	5.66 ± 2.98
303	6.0	116	236	1.2	36.0	44	16.8	2.2	201	5.57 ± 2.93
400	12.0	119	75	1.2	16.5	43	29.4	−9.4	82.0	4.98 ± 1.76
450	6.0	113	228	1.2	58.3	44	37.8	4.3	290	4.98 ± 1.18
600	6.0	114	264	1.0	73.2	38	27.3	0.7	398	5.44 ± 0.87
600	12.0	128	103	1.1	27.7	37	33.1	4.2	117	4.23 ± 0.96
600	12.0	125	190	1.1	51.1	37	13.8	−20.8	231	4.53 ± 1.40
800	6.0	112	277	1.1	88.2	41	25.6	2.3	433	4.91 ± 0.75
800	12.0	131	212	1.2	61.1	37	51.8	−2.7	237	3.88 ± 0.93
800	12.0	80	264	0.27	29.2	14	36.8	−5.5	114	3.92 ± 0.76

[a] Concentration of the bath gas (helium) in units of 10^{16} atom cm^{-3}. [b] In units of 10^{11} molecule cm^{-3}. Concentration of CH_2Cl is an upper limit (see text). [c] Laser intensity in mJ $pulse^{-1}$ cm^{-2}. [d] Small negative values of k_9 observed in some of the experiments can be attributed to slight imperfections in the relative alignment of the reactor and the photolyzing laser beam. [e] In units of 10^{-11} cm^3 $molecule^{-1}$ s^{-1}.

TABLE 2: Conditions and Results of Experiments to Determine the Rate Constants k_2 of the $CHCl_2 + CH_3$ Reaction

T/K	[He][a]	$[CHCl_3]$[b]	$[C_3H_6O]$[b]	$[CHCl_2]_0$ [b]	$[CH_3]_0$ [b]	I[c]	k_8/s^{-1}	k_9/s^{-1} [d]	$k_6[CH_3]_0/s^{-1}$	k_2 [e]
304	6.0	151	181	0.7	20.7	21	35.7	−1.9	115.1	5.55 ± 1.37
304	6.0	151	332	0.3	14.6	8	23.3	−1.0	86.9	5.95 ± 1.55
304	6.0	151	380	0.7	40.7	20	27.7	−1.7	213.9	5.24 ± 1.82
400	6.0	39	121	0.3	25.8	37	32.9	2.7	82.2	3.19 ± 1.53
400	6.0	158	260	0.9	39.8	26	50.8	4.7	159.1	4.01 ± 1.25
600	6.0	37	74	0.3	19.4	33	14.7	5.0	54.0	2.79 ± 0.54
600	12.0	43	111	0.3	27.9	33	20.7	4.0	78.4	2.81 ± 0.83
800	6.0	36	62	0.2	17.4	30	17.2	0.0	37.1	2.13 ± 0.33
800	6.0	36	112	0.1	12.9	12	11.1	19.0	45.9	3.55 ± 1.13
800	12.0	180	147	1.0	34.2	24	18.5	21.4	85.8	2.51 ± 0.98
800	12.0	119	276	0.3	29.3	11	10.7	6.6	94.8	3.23 ± 0.51

[a] Concentration of the bath gas (helium) in units of 10^{16} atom cm^{-3}. [b] In units of 10^{11} molecule cm^{-3}. Concentration of $CHCl_2$ is an upper limit (see text). [c] Laser intensity in mJ $pulse^{-1}$ cm^{-2}. [d] Small negative values of k_9 observed in some of the experiments can be attributed to slight imperfections in the relative alignment of the reactor and the photolyzing laser beam. [e] In units of 10^{-11} cm^3 $molecule^{-1}$ s^{-1}.

experiments. The error limits of the experimentally obtained rate constant values reported in this work represent a sum of 2σ statistical uncertainty (on average, 22% of k_i) and estimated systematic uncertainty (on average, 7% of k_i).

Experimental Results. The rate constants of reactions 1 and 2 were determined at temperatures between 301 and 800 K and bath gas densities $[He] = (6-12) \times 10^{16}$ atom cm^{-3}. The upper limit of the experimental temperatures was determined by the onsets of thermal decomposition of CH_2Cl_2 and $CHCl_3$. Conditions and results of all experiments are listed in Tables 1 and 2. It was verified experimentally that these rate constants did not depend on the photolyzing laser intensity, initial concentrations of R and CH_3, or concentrations of the photolytic precursors. The rate constants of reactions 1 and 2 did not demonstrate any pressure dependence within the experimental uncertainties.

Arrhenius plots of the rate constants of reaction 1 and 2 are shown in Figures 3 and 4. These temperature dependences can be represented with the following expressions

$$k_1 = 3.93 \times 10^{-11} \exp(91\ \mathrm{K/T})\ \mathrm{cm^3\ molecule^{-1}\ s^{-1}} \quad \text{(III)}$$

$$k_2 = 1.66 \times 10^{-11} \exp(359\ \mathrm{K/T})\ \mathrm{cm^3\ molecule^{-1}\ s^{-1}} \quad \text{(IV)}$$

The estimated uncertainties of these expressions are 25%. Experimental error limits of individual data points are given in Tables 1 and 2.

The observed rate constants of reaction 1 demonstrate very little dependence on temperature, with the differences between the values obtained at different temperatures being well within the ranges of experimental uncertainties (Figure 3). If the values of k_1 obtained at different temperatures are averaged, one obtains

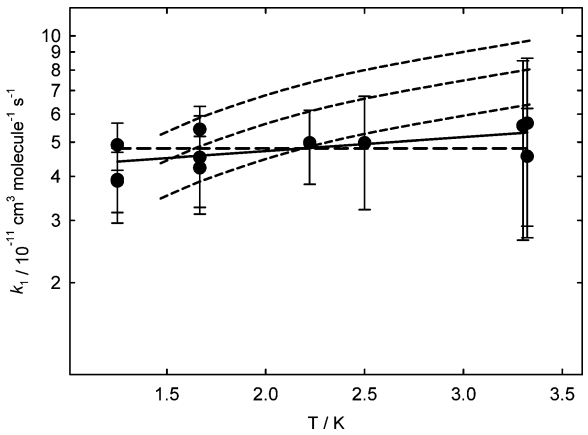

Figure 3. Temperature dependence of the rate constant of the $CH_2Cl + CH_3$ reaction, k_1. Experimental values are shown by symbols. The solid line is Arrhenius expression of eq III. The long-dashed line represents the temperature-independent value of eq V. Three short-dashed lines show the central and the limiting values of k_1 calculated using the "geometric mean rule," eq VI.

a temperature-independent value

$$k_1 = (4.8 \pm 0.7) \times 10^{-11}\ \mathrm{cm^3\ molecule^{-1}\ s^{-1}}\ (301-800\ \mathrm{K}) \quad \text{(V)}$$

The uncertainty of the k_1 value in equation V (smaller than the error limits of individual determinations listed in Table 1) is composed by adding the 2σ statistical uncertainty resulting from averaging and the 8.8% average systematic component of the uncertainty of rate determination. This averaging, certainly, is meaningful only under the assumption of the true temperature independence of k_1, i.e., if it is assumed that k_1 is intrinsically

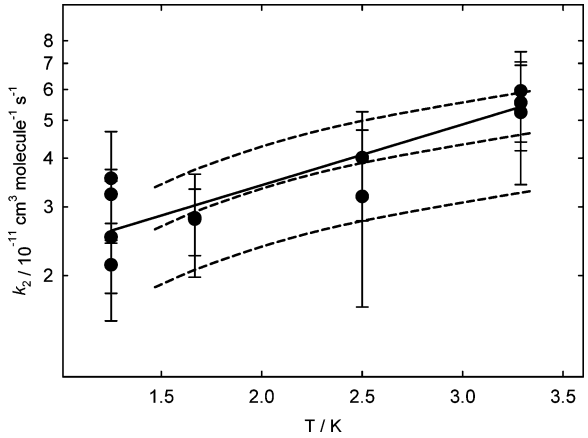

Figure 4. Temperature dependence of the rate constant of the $CHCl_2 + CH_3$ reaction, k_2. Experimental values are shown by symbols. The solid line is Arrhenius expression of eq IV. Three dashed lines show the central and the limiting values of k_2 calculated using the "geometric mean rule," eq VI.

independent of temperature, as opposed to a case of a weak temperature dependence masked by the experimental uncertainties and data scatter.

Formation of C_2H_4 and C_2H_3Cl was detected in the experiments on reactions 1 and 2, respectively, at both the low and the high ends of the experimental temperature intervals. The signal growth profiles of these products matched the decay of the corresponding R radicals, which is illustrated in the insets in Figures 1 and 2 with solid lines obtained in kinetic modeling of product growth using the mechanisms of reactions 1 (2), 6, 7 (8), and 9 and the rate parameters derived from the R and CH_3 decay profiles. The following potential reaction products were searched for but not found: C_2H_5 and C_2H_5Cl in reaction 1 and CH_3CHCl and $C_2H_4Cl_2$ in reaction 2.

In principle, CH_3 decay profiles observed in the experiments can be used to derive the values of k_6. However, the experimental conditions used in the current study were optimized for most accurate determination of k_1 and k_2, not k_6. As a result, the derived values of k_6 have large uncertainties precluding any meaningful comparison with the results of previous determinations. Thus, no attempts at such an analysis were made, except for the verification that the uncertainty ranges of k_6 overlap with those of earlier studies.[11−14,22]

$CH_2Cl + O_2$ and $CHCl_2 + O_2$ Reactions at 800 K. A separate short study of the high-temperature reactions between R (R = CH_2Cl or $CHCl_2$) and O_2

$$CH_2Cl + O_2 \rightarrow \text{products} \quad (10)$$

$$CHCl_2 + O_2 \rightarrow \text{products} \quad (11)$$

was attempted at 800 K. The experimental conditions were similar to those used in the main part of this work, except for the absence of acetone and CH_3. No reaction could be detected. Upper limit values of k_{10}, $k_{11} \leq 1.2 \times 10^{-16}$ cm^3 molecule^{-1} s^{-1} were obtained by adding up to 3×10^{16} molecules cm^{-3} of O_2. (The concentration of He was reduced accordingly so that the total concentration of bath gas, $[He] + [O_2] = 1.2 \times 10^{17}$ molecules cm^{-3}, remained constant.)

III. Discussion

This work presents the first experimental determination of the rate constants of reactions 1 and 2. No earlier data exist in the literature. In general, reliable rate data on radical−radical reactions are sparse as these reactions are difficult to study experimentally due to the high reactivity of the chemical species involved. Because of the lack of directly obtained experimental values, rate constants of cross-combination reactions are often estimated using the "geometric mean rule".[10,23,24]

$$k_{AB} = 2(k_{AA}k_{BB})^{1/2} \quad (VI)$$

(Here k_{AB} is the rate constant of the A + B reaction and k_{AA} and k_{BB} are the rate constants of the A + A and B + B self-reactions, respectively.)

It is instructive to use the experimental temperature dependence of the rate constant of reactions 1 and 2 to examine the performance of the "geometric mean rule" for the reactions of chlorinated methyl radicals with CH_3. The rate constants of the methyl radical self-reaction (reaction 6) are well known. Two recent "global fits"[25,26] of falloff data provide parametrization for the rate constants that differ very little (less than 5%) in the high-pressure limit. A large part of the experimental data used in these parametrizations comes from the experimental study of Slagle et al.[22] who used the experimental technique and the apparatus analogous to that employed in the current work. These authors reported a ±20% uncertainty in their experimental rate constant values. Thus, in the calculations according to the "geometric mean rule," we used the parametrization of Hessler and Ogren[26] ($k_6^\infty(298\ K) = 5.81 \times 10^{-11}$ cm^3 molecule^{-1} s^{-1}) with 20% uncertainty. The high-pressure limit rate constants of the self-reactions of $CHCl_2$ and CH_2Cl radicals

$$CH_2Cl + CH_2Cl \rightarrow CH_2ClCH_2Cl \text{ (or } HCl + C_2H_3Cl) \quad (12)$$

$$CHCl_2 + CHCl_2 \rightarrow CHCl_2CHCl_2 \text{ (or } HCl + C_2HCl_3) \quad (13)$$

have been determined by Roussel et al.[27] in their flash photolysis/kinetic UV spectroscopy study in the 273−683-K temperature range. These authors reported $k_{12}(T) = 2.8 \times 10^{-11}$ $(T/298\ K)^{-0.85}$ cm^3 molecule^{-1} s^{-1} and $k_{13}(T) = 6.3 \times 10^{-10}$ $(T/298\ K)^{-0.74}$ cm^3 molecule^{-1} s^{-1} temperature dependences. The 1σ uncertainties of the temperature independent prefactors reported by Roussel et al. are 10.5 and 18.5% for k_{12} and k_{13}, respectively, which includes the uncertainties due to those of the UV cross sections of $CHCl_2$ and CH_2Cl. Therefore, we use the expressions of ref 27 for k_{12} and k_{13} with the 2σ overall uncertainties of 21 and 37%.

The resultant k_1 and k_2 temperature dependences calculated via eq VI (the "geometric mean rule") using the literature values of k_6, k_{12}, and k_{13} are shown in Figures 3 and 4. The upper and the lower limiting values were calculated using the upper and the lower limits of k_6, k_{12}, and k_{13}. The calculated $k_1(T)$ and $k_2(T)$ dependences are in reasonable agreement with the experimental values obtained in this work over the ranges of temperatures where information on both k_{12} and k_{13} is available.

Both reactions 1 and 2 can proceed via three product channels, all involving formation of an excited $R-CH_3$* intermediate

$$CH_2Cl + CH_3 \rightarrow CH_2ClCH_3^* \rightarrow HCl + C_2H_4 \quad (1a)$$

$$\rightarrow Cl + C_2H_5 \quad (1b)$$

$$\rightarrow C_2H_5Cl \quad (1c)$$

$$CHCl_2 + CH_3 \rightarrow CHCl_2CH_3^* \rightarrow HCl + C_2H_3Cl \quad (2a)$$

$$\rightarrow Cl + CH_3CHCl \quad (2b)$$

$$\rightarrow CHCl_2CH_3 \quad (2c)$$

In the current study, only products of the chemically activated routes 1a and 2a (C_2H_4 and C_2H_3Cl) were observed, indicating that, under the experimental conditions used, channels of collisional stabilization and adduct decomposition via Cl atom elimination are negligible.

Experimental studies of C_2H_5Cl and $CHCl_2CH_3$ pyrolysis report activation energies of $\sim 53-57$ kcal mol^{-1} for thermal decomposition via HCl elimination pathways (e.g., refs 28−32). These barriers, combined with known heats of formation of the species involved,[33−35] translate into a $\sim$32−35 kcal mol^{-1} gap between the entrance and the exit barriers in reaction channels 1a and 2a. These large differences between the entrance and the exit barriers mean that any pressure dependences of the overall $CHCl_2 + CH_3$ and $CH_2Cl + CH_3$ reactions are highly unlikely since all vibrationally excited adducts will either decompose to the products of channels 1a or 2a or stabilize by collisions with the bath gas. The absence of an observable pressure dependences of k_1 and k_2 is in agreement with this conclusion.

High-Temperature $CH_2Cl + O_2$ and $CHCl_2 + O_2$ Reactions. At low temperatures, the main channel of the reactions of chlorinated methyl radicals with O_2 is reversible addition to form an RO_2 peroxy radical ($R + O_2 \rightarrow RO_2$). The reactions of CH_2Cl and $CHCl_2$ with O_2 have been extensively studied experimentally in both the low-temperature (addition) and the intermediate-temperature (relaxation to equilibrium) regions.[36−38] However, no rate constant measurements have been reported at higher temperatures, where equilibrium in the addition step is shifted to the left and the overall reaction (if any) is dominated by the rearrangement of the excited peroxy adduct. Ho et al.[4,39] studied the high-temperature reaction of chloromethyl radical with O_2

$$CH_2Cl + O_2 \rightleftarrows CH_2ClOO \rightarrow CH_2O + ClO \qquad (10)$$

using the computational QRRK method; their estimated temperature dependence of k_{10} results in the value of $k_{10} \approx 6 \times 10^{-14}$ cm^3 molecule^{-1} s^{-1} at 800 K. The mechanism of the reaction of $CHCl_2$ with O_2 at high temperatures can be expected to be similar. The results of the current study demonstrate that, if such reactions take place, their rate constant at 800 K are at least 2 orders of magnitude lower than the estimate of refs 4 and 39 for reaction 10. Similarly, in our earlier study[11] an upper limit of 3.0×10^{-16} cm^3 molecule^{-1} s^{-1} was obtained for the 800 K rate constant of the reactions of CCl_3 with O_2.

Acknowledgment. This research was supported by the National Science Foundation, Combustion and Thermal Plasmas Program under Grant No. CTS-0105239.

References and Notes

(1) Tsang, W.; Hampson, R. F. *J. Phys. Chem. Ref. Data* **1986**, *15*, 1087.
(2) Warnatz, J. In *Combustion Chemistry*; Gardiner, W. C. Jr., Ed.; Springer-Verlag: New York, 1984.
(3) Knyazev, V. D.; Slagle, I. R. *J. Phys. Chem. A* **1998**, *102*, 1770.
(4) Ho, W. P.; Yu, Q.-R.; Bozzelli, J. W. *Combust. Sci. Technol.* **1992**, *85*, 23.
(5) Qun, M.; Senkan, S. M. *Combust. Sci. Technol.* **1994**, *101*, 103.
(6) Tavakoli, J.; Chiang, H. M.; Bozzelli, J. W. *Combust. Sci. Technol.* **1994**, *101*, 135.
(7) Karra, S. B.; Senkan, S. M. *Ind. Eng. Chem. Res.* **1988**, *27*, 447.
(8) Granada, A.; Karra, S. B.; Senkan, S. M. *Ind. Eng. Chem. Res.* **1987**, *26*, 1901.
(9) Garland, L. J. Ph.D. Dissertation, University of California at Los Angeles: Los Angeles, California, 1989.
(10) Garland, L. J.; Bayes, K. D. *J. Phys. Chem.* **1990**, *94*, 4941.
(11) Knyazev, V. D.; Slagle, I. R.; Bryukov, M. G. *J. Phys. Chem. A* **2003**, *107*, 6558.
(12) Stoliarov, S. I.; Knyazev, V. D.; Slagle, I. R. *J. Phys. Chem. A* **2000**, *104*, 9687.
(13) Knyazev, V. D.; Slagle, I. R. *J. Phys. Chem. A* **2001**, *105*, 3196.
(14) Knyazev, V. D.; Slagle, I. R. *J. Phys. Chem. A* **2001**, *105*, 6490.
(15) Slagle, I. R.; Gutman, D. *J. Am. Chem. Soc.* **1985**, *107*, 5342.
(16) Krasnoperov, L. N.; Niiranen, J. T.; Gutman, D.; Melius, C. F.; Allendorf, M. D. *J. Phys. Chem.* **1995**, *99*, 14347.
(17) Daly, N. R. *Rev. Sci. Insrum.* **1960**, *31*, 264.
(18) Okabe, H. *Photochemistry of Small Molecules*; Wiley: New York, 1978.
(19) Lightfoot, P. D.; Kirwan, S. P.; Pilling, M. J. *J. Phys. Chem.* **1988**, *92*, 4938.
(20) Niiranen, J. T.; Gutman, D. *J. Phys. Chem.* **1993**, *97*, 9392.
(21) Bevington, P. R. *Data Reduction and Error Analysis for the Physical Sciences*; McGraw-Hill: New York, 1969.
(22) Slagle, I. R.; Gutman, D.; Davies, J. W.; Pilling, M. J. *J. Phys. Chem.* **1988**, *92*, 2455.
(23) Kerr, J. A.; Trotman-Dickenson, A. F. *Prog. React. Kinet.* **1961**, *1*, 105.
(24) Blake, A. R.; Henderson, J. F.; Kutschke, K. O. *Can. J. Chem.* **1961**, *39*, 1920.
(25) Robertson, S. H.; Pilling, M. J.; Baulch, D. L.; Green, N. J. B. *J. Phys. Chem.* **1995**, *99*, 13452.
(26) Hessler, J. P.; Ogren, P. J. *J. Phys. Chem.* **1996**, *100*, 984.
(27) Roussel, P. B.; Lightfoot, P. D.; Caralp, F.; Catoire, V.; Lesclaux, R.; Forst, W. *J. Chem. Soc., Faraday Trans.* **1991**, *87*, 2367.
(28) Tsang, W. *J. Chem. Phys.* **1964**, *41*, 2487.
(29) Shilov, A. E.; Sabirova, R. D. *Kinet. Catal.* **1964**, *5*, 32.
(30) Evans, P. J.; Ichimura, T.; Tschuikow-Roux, E. *Int. J. Chem. Kinet.* **1978**, *10*, 855.
(31) Holbrook, K. A.; Marsh, A. R. W. *Trans. Faraday Soc.* **1967**, *63*, 643.
(32) Jonas, R.; Heydtmann, H. *Ber. Bunsen-Ges. Phys. Chem.* **1978**, *82*, 823.
(33) Kerr, J. A. *CRC Handbook of Chemistry and Physics*, 75th ed.; Lide, D. R., Ed.; *CRC Press*: Boca Raton, FL, 1995.
(34) Cox, J. D.; Pilcher, G. *Thermochemistry of Organic and Organometallic Compounds*; Academic Press: New York, 1970.
(35) Fletcher, R. A.; Pilcher, G. *Trans. Faraday Soc.* **1971**, *67*, 3191.
(36) Fenter, F. F.; Lightfoot, P. D.; Caralp, F.; Lesclaux, R.; Niiranen, J. T.; Gutman, D. *J. Phys. Chem.* **1993**, *97*, 4695.
(37) Bilde, M.; Sehested, J.; Nielsen, O. J.; Wallington, T. J.; Meagher, R. J.; McIntosh, M. E.; Piety, C. A.; Nicovich, J. M.; Wine, P. H. *J. Phys. Chem. A* **1997**, *101*, 8035.
(38) Nottingham, W. C.; Rudolph, R. N.; Andrews, K. P.; Moore, J. H.; Tossell, J. A. *Int. J. Chem. Kinet.* **1994**, *26*, 749.
(39) Ho, W. P.; Barat, R. B.; Bozzelli, J. W. *Combust. Flame* **1992**, *88*, 265.